Canadian Mineralogist
Vol. 24, pp. 649-654 (1986)

RE-EVALUATION OF ORDERING AND LOCAL CHARGE-BALANCE IN Ia CHLORITE

STURGES W. BAILEY
Department of Geology and Geophysics, University of Wisconsin-Madison, Madison, Wisconsin 53706, U.S.A.

ABSTRACT

In 1963 a structural refinement, by film methods, of a triclinic 1-layer chromian chlorite of the I*a* structural type claimed long-range ordering of both the tetrahedrally co-ordinated Si,Al cations and the octahedrally co-ordinated R^{3+}, R^{2+} cations in the interlayer sheet. Refinement by modern methods (R = 4.4%) of the same crystal confirms the ordering of octahedral cations but not that of the tetrahedral cations. This result implies that charge balance between ordered sources of net negative and positive charges on layer and interlayer, postulated by the earlier authors, cannot exist and thus cannot mitigate the cation–cation repulsion geometrically inherent in *a*-type superpositions. Other authors have shown that an earlier interpretation of similar charge-balance in ordered 1*a* vermiculite is likewise incorrect, although in this case short-range ordering of both kinds of cations is present in some specimens. These observations raise the possibility that charge balance may exist either within or between small ordered domains in *a* structures. Such charge balance can only be a minor factor in influencing chlorite stability, however, because it cannot occur in the more abundant chlorites of the *b*-type structures, in which nearest-neighbor cations in layer and interlayer do not directly superimpose.

Keywords: chlorite, vermiculite, cation ordering, charge balance.

SOMMAIRE

En 1963, un affinement de la structure d'une chlorite à chromium, triclinique, à une couche, du type I*a*, annonçait l'ordre à longue distance tant des cations (Si,Al) tétraédriquement coordonnés que des cations (R^{3+}, R^{2+}) du feuillet inter-couches. L'affinement par méthodes modernes (R = 4.4%) du même cristal confirme l'ordre des cations octaédriques, mais non celui des cations tétraédriques. Ce résultat implique que la neutralisation des charges entre sources ordonnées de charges nettes positive et négative sur couche et inter-couche, qui est postulée par les travaux antérieurs, ne peut pas exister et ne peut donc pas mitiger la répulsion inter-cations géométriquement inhérente aux superpositions du type *a*. D'autres auteurs ont montré qu'une interprétation antérieure d'un semblable bilan des charges dans la vermiculite ordonnée I*a* était elle aussi incorrecte (quoique, en ce cas, l'ordre à courte distance des cations des deux sortes ait été observé dans quelques spécimens). Ces observations rendent possible la neutralisation des charges à l'intérieur de petits domaines ordonnés, ou entre de tels domaines, dans les structures du type *a*. Pareille neutralisation, cependant, ne peut guère influencer la stabilité d'une chlorite, étant donné qu'elle en peut pas se produire dans les chlorites du type *b*, les plus abondantes, dans lesquelles des cations proche voisins dans couche et inter-couches ne se trouvent pas directement l'un audessus de l'autre.

(Traduit par la Rédaction)

Mots-clés: chlorite, vermiculite, cations ordonnés, bilan des charges.

INTRODUCTION

Bailey & Brown (1962) showed that the interlayer sheets in chlorite or vermiculite may be oriented to have either the same (I) or opposite (II) slant to that of the sheet of octahedra within the 2:1 layer portion of the structure. The interlayer may then be positioned by hydrogen bonds so that the interlayer cations either do (*a*) or do not (*b*) superimpose on tetrahedrally co-ordinated cations in the sheet of tetrahedra below (Fig. 1). Interlayer orientations I and II are related to each other by 180° or ±60° rotations, and positions *a* and *b* to each other by a shift of *a*/3. Layer–interlayer assemblages thus may be termed I*a*, I*b*, II*a* and II*b*. Depending on the positioning of the hydrogen bonds leading to the 2:1 layer above the interlayer sheet, the I*b* and II*a* chlorites with regular one-layer structures or with semirandom layer-sequences may have either resultant orthorhombic-shaped ($\beta = 90°$) but monoclinic-symmetry unit cells, monoclinic-shaped ($\beta = 97°$) and monoclinic- or triclinic-symmetry cells, or triclinic-shaped (α = 102°) and triclinic-symmetry cells. I*a* and II*b* chlorites, on the other hand, always have monoclinic-shaped cells unless cation ordering distorts the cell shape. The position of the second 2:1 layer can be stated more exactly in the symbol by adding a number (1 to 6) that specifies the location of the centre of its lower hexogonal ring relative to the symmetry plane of the first 2:1 layer. Thus, numbers 1 and 2 indicate that the lower ring lies on the symmetry plane to give resulting monoclinic symmetry, whereas numbers 3 to 6 indicate asymmetrical positions and resultant triclinic symmetry.

The different sequences of sheets that are possible lead to different amounts of cation–cation repulsion and cation–anion attraction. These have been evaluated by Bailey & Brown (1962) and Shirozu & Bailey (1965) and correlated with the observed abundances of the different structural types of chlorite. These authors concluded that repulsion between tetrahedral

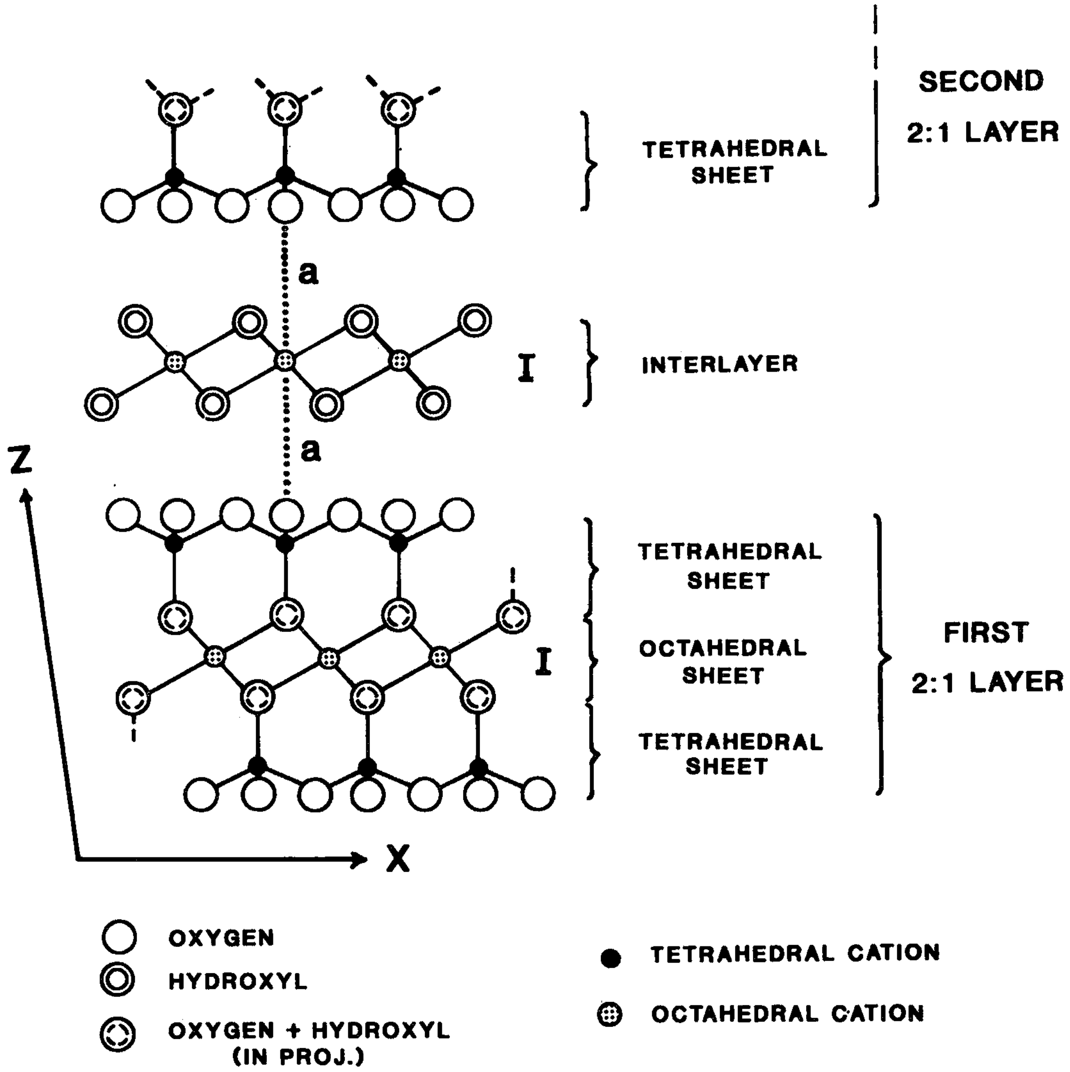

FIG. 1. *XZ* projection of I*a* structure of chlorite. I signifies that the octahedra in the interlayer sheet slant in the same direction as those in the 2:1 layer. II. signifies opposite slants. An interlayer cation in position *a* causes superposition of tetrahedral and interlayer cations (vertical dotted line). Position *b* (not shown) shifts the interlayer by *a*/3 so that this cation–cation repulsion is avoided.

and interlayer cations is the most important structural factor in reducing the stabilities of I*a* and II*a* arrangements relative to those of I*b* and II*b*. No examples of II*a* chlorite have yet been recognized in nature, and I*a* chlorite is less abundant than I*b* and II*b*. Note that II*b* structures are more stable than I*b* structures because rotation of tetrahedra to alleviate lateral misfit between tetrahedral and octahedral sheets in the 2:1 layer and to shorten hydrogen-bond contacts between layer and interlayer moves the basal oxygen atoms closer to the 2:1 octahedral cations in the II*b* structure, as in all micas, but farther away in the I*b* structure. The same is true of the I*a* structure relative to II*a* and, in fact, the I*a* structure would be extremely stable were it not for the cation–cation repulsion noted above. It is notable that when this repulsion is minimized by having only a small number of interlayer cations present, as in vermiculite, the structural form is always I*a*.

Crystal-structure refinements by film techniques two decades ago indicated long-range ordering of both tetrahedral and interlayer cations for a 1-layer I*a*–4 chromian chlorite from Erzincan, Turkey (Brown & Bailey 1963), and for a 2-layer I*a* vermiculite from

Llano County, Texas (Shirozu & Bailey 1966). Local charge-balance also was found in which the ordered source of net positive charge on the interlayer sheet was positioned on a vertical line between the ordered sources of net negative charge on the tetrahedral sheets immediately above and below (Fig. 1). It was suggested that this ordering and local charge-balance conferred an additional measure of stability to the *I*a structure by partially mitigating the repulsion factor.

Since then, de la Calle *et al.* (1976) have shown that the density of $\pm b/3$ stacking faults is so large in the Llano vermiculite that the alternation of $+b/3$ and $-b/3$ layer shifts required in the ideal 2-layer structure is not sufficiently regular to permit determination of ordering by X-ray study. Thompson (1984) studied the same material by NMR and concluded that there may be some short-range ordering of tetrahedral Si and Al, but no long-range ordering.

There are no $\pm b/3$ stacking faults in the I*a*–4 Erzincan chlorite, but the structure was determined initially by Weissenberg film methods using only *hk*0, 0*kl*, and *h*0*l* intensity data in a diagonal-term least-squares refinement ($R =$ 10.3%). A more accurate refinement by modern techniques is reported here in order to assess the validity of the earlier study and the importance of local charge-balance in I*a* structures.

EXPERIMENTAL

Brown & Bailey (1963) used two different crystals to obtain intensity data. One of the two crystals was still available and was used in this study. It is in the shape of a 4-sided slice 0.21 × 0.14 × 0.14 × 0.10 mm on the sides and 0.12 mm thick. Unit-cell dimensions [a 5.329(1), b 9.246(2), c 14.442(5) Å, α 90.00(2)°, β 97.08(3)°, and γ 90.04(2)°] were determined by least-squares fit of 15 low- to medium-angle reflections on a Nicolet $P2_1$ automated single-crystal diffractometer. Reflection intensities were collected in all octants out to $2\theta = 60°$ with graphite-monochromated Mo$K\alpha$ radiation in the θ:2θ variable-scan mode. One standard reflection was checked after every 50 reflections in order to monitor crystal and electronic stability. No instability was noted. Integrated intensities, corrected for background, were corrected for Lp effects and for absorption by the semi-empirical psi-scan method of North *et al.* (1968). Friedel equivalents were averaged to give a set of 1606 nonequivalent reflections. The space group is triclinic $C\bar{1}$, based on the intensity relationships and an N(z) statistical test for a centre of symmetry. Thus, the structure is confirmed as I*a*–4 (equivalent to I*a*–6). The sense (+ or –) of the k indices was determined by comparison of F_o values with those calculated from the Brown & Bailey I*a*–4 structure.

The starting atomic co-ordinates for refinement were those of the I*a*–4 structure from Brown & Bailey, with fixed isotropic B values of 0.5 for T cations, 0.8 for M cations, and 1.2 for anions. The composition was assumed to be $(Mg_{5.0}Fe_{0.1}Cr_{0.7}Al_{0.2})(Si_{3.0}Al_{1.0})O_{18}H_{7.9}$, as given by Brown & Bailey (1963). Scattering factors appropriate for 50% ionization and cation disorder were taken from Cromer & Mann (1968). Non-fixed atomic co-ordinates and the scale factor were varied first in repeated cycles of least-squares fit with a modified ORFLS program. After convergence, the scattering factors were adjusted to fit the ordering of interlayer cations indicated by bond lengths and difference electron-density maps. Isotropic and then anisotropic temperature-parameters were added as variables in refinement. After reducing the residual R to a minimum the H^+ protons of all of the OH groups were located as volumes of excess density (0.3 to 0.6 electrons) on difference electron-density maps. Their positions were not refined, but their contributions to the F_c values were included. The final residual R was 4.4%. Unit weights were used throughout because of our experience that these are better than sigma weights for the intensity distributions found in phyllosilicates.

TABLE 1. ATOMIC POSITIONS

	x	y	z	B equiv
T(1)	0.3968(2)	-0.0001(1)	0.1906(1)	0.648
T(2)	0.8970(2)	0.1667(1)	0.1908(1)	0.686
M(1)	0.0	0.0	0.0	0.536
M(2)	-0.0009(2)	0.3334(1)	0.00006(9)	0.555
M(3)	0.0012(2)	0.1666(1)	0.50314(9)	0.430
M(4)	0.5	0.0	0.5	0.949
O(1)	0.3590(5)	0.0000(3)	0.0766(2)	0.679
O(2)	0.8588(5)	0.1667(3)	0.0767(2)	0.703
OH(1)	0.3578(5)	0.3331(3)	0.0734(2)	0.796
O(3)	0.1467(6)	0.0691(3)	0.2319(2)	1.410
O(4)	0.6463(6)	0.0967(3)	0.2318(2)	1.470
O(5)	0.9383(6)	0.3333(3)	0.2320(2)	1.399
OH(2)	0.1517(5)	0.0018(3)	0.4291(2)	0.958
OH(3)	0.1359(5)	0.3368(3)	0.4292(2)	0.980
OH(4)	0.6415(5)	0.1616(3)	0.4292(2)	0.982
H(1)	0.3670	0.3314	0.1405	
H(2)	0.0968	0.0189	0.3714	
H(3)	0.0816	0.3356	0.3681	
H(4)	0.6181	0.1525	0.3730	

TABLE 2. ANISOTROPIC THERMAL PARAMETERS*

	β_{11}	β_{22}	β_{33}	β_{12}	β_{13}	β_{23}
T(1)	54(3)	14(1)	10.5(5)	1(1)	3(1)	0.8(5)
T(2)	58(3)	15(1)	10.9(5)	-1(1)	3(1)	0.5(5)
M(1)	39(3)	11(2)	9.7(8)	-0(2)	3(2)	0.4(9)
M(2)	41(4)	12(1)	9.7(5)	1(2)	2(1)	0.4(6)
M(3)	36(4)	6(1)	8.3(5)	0(1)	2(1)	0.4(6)
M(4)	88(3)	23(1)	13.1(5)	0(1)	4(1)	0.7(5)
O(1)	45(8)	16(3)	12(1)	4(3)	4(2)	1(1)
O(2)	41(8)	17(3)	13(1)	0(3)	4(2)	1(1)
OH(1)	60(9)	19(3)	13(1)	-1(4)	4(2)	0(1)
O(3)	121(10)	46(3)	16(1)	16(4)	6(3)	2(2)
O(4)	132(11)	48(3)	16(1)	-15(5)	3(3)	-0(2)
O(5)	162(11)	32(3)	16(1)	3(4)	5(3)	1(2)
OH(2)	113(10)	24(3)	10(1)	3(4)	4(3)	1(1)
OH(3)	109(10)	26(3)	10(1)	-4(4)	3(3)	0(1)
OH(4)	97(9)	27(3)	11(1)	3(4)	5(3)	-0(1)

$^*\beta_{ij}=\beta_{ij}\times 10^4$

TABLE 3. ORIENTATION OF ANISOTROPIC THERMAL ELLIPSOIDS

Atom	Axis	RMS Displacement	Angle in Degrees with respect to X	Y	Z
T(1)	r1	0.078(3)	80(13)	168(11)	84(4)
	r2	0.088(3)	11(12)	79(13)	95(6)
	r3	0.105(2)	87(6)	96(4)	173(5)
T(2)	r1	0.079(3)	95(11)	174(8)	86(4)
	r2	0.091(3)	9(8)	94(11)	89(7)
	r3	0.107(2)	82(7)	94(4)	176(4)
M(1)	r1	0.068(5)	98(39)	171(36)	86(8)
	r2	0.074(5)	8(38)	98(39)	97(8)
	r3	0.101(4)	91(8)	93(7)	172(8)
M(2)	r1	0.071(3)	74(31)	163(31)	88(5)
	r2	0.076(3)	17(30)	74(31)	93(6)
	r3	0.100(3)	85(6)	93(5)	176(5)
M(3)	r1	0.050(5)	90(9)	177(4)	87(4)
	r2	0.071(4)	3(7)	90(9)	94(7)
	r3	0.093(3)	87(6)	93(4)	175(6)
M(4)	r1	0.099(2)	91(8)	172(6)	82(6)
	r2	0.112(2)	4(22)	90(8)	93(22)
	r3	0.117(2)	86(23)	98(6)	172(11)
O(1)	r1	0.074(7)	36(27)	126(26)	91(9)
	r2	0.087(7)	54(27)	37(26)	101(10)
	r3	0.114(6)	90(9)	98(9)	169(10)
O(2)	r1	0.076(8)	177(24)	88(29)	85(8)
	r2	0.087(6)	88(29)	5(17)	94(10)
	r3	0.114(5)	88(8)	94(10)	173(9)
OH(1)	r1	0.088(7)	118(98)	153(98)	86(12)
	r2	0.091(7)	28(98)	118(98)	94(12)
	r3	0.118(6)	89(10)	91(9)	174(10)
O(3)	r1	0.120(6)	39(16)	125(8)	80(26)
	r2	0.130(5)	111(22)	92(18)	14(21)
	r3	0.152(5)	122(9)	145(8)	99(12)
O(4)	r1	0.124(6)	133(25)	119(21)	117(44)
	r2	0.130(5)	113(34)	113(25)	29(42)
	r3	0.154(5)	52(9)	142(9)	98(10)
O(5)	r1	0.117(6)	87(7)	169(17)	80(18)
	r2	0.132(6)	88(13)	79(18)	14(16)
	r3	0.152(5)	176(9)	93(8)	81(12)
OH(2)	r1	0.100(6)	85(11)	170(30)	83(36)
	r2	0.107(6)	94(15)	82(36)	8(33)
	r3	0.125(6)	173(12)	96(11)	86(15)
OH(3)	r1	0.103(6)	104(12)	163(38)	79(59)
	r2	0.107(6)	92(21)	80(57)	11(57)
	r3	0.124(6)	166(12)	77(12)	87(15)
OH(4)	r1	0.106(6)	69(27)	159(29)	94(41)
	r2	0.113(6)	106(63)	99(45)	12(63)
	r3	0.117(6)	153(46)	109(27)	101(66)

The final atomic positions and anisotropic thermal parameters are listed in Tables 1–3. Bond lengths and errors calculated by program ORFFE are given in Table 4. Table 5 lists other structural parameters. A table of F_o and F_c values can be obtained at nominal charge from the Depository of Unpublished Data, CISTI, National Research Council of Canada, Ottawa, Ontario K1A 0S2.

Discussion

The triclinic symmetry of the I*a*-4 structure arises because the *a*/3 shifts within successive 2:1 layers are not collinear (as signified by the symbol 4). Relative to pseudohexagonal axes, there is a shift of $-0.334a_3$ within each 2:1 layer. But the entire second 2:1 layer is shifted by $-0.334a_1$ relative to the first layer so that the unit-cell shape (as contrasted to its symmetry) is monoclinic.

The two nonequivalent tetrahedra are nearly identical (the mean *T*–O values are 1.650 and 1.652 Å), rather than being ordered as originally claimed. There is no ordering of octahedral cations (entirely Mg) within the 2:1 layer (the mean *M*–O,OH values are 2.083 and 2.081 Å), but all of the trivalent Cr + Al atoms (0.9) are preferentially ordered on a centre of symmetry in interlayer site *M*(4) relative to *M*(3) according to bond lengths (mean *M*–OH 2.007 *versus* 2.068 Å) and difference electron-density maps. The *M*(3) site is occupied entirely by Mg cations. All of the octahedral bond-lengths are close to those determined by Brown & Bailey (1963), but the tetrahedral bond-lengths in the two studies differ by 0.02 to 0.04 Å. Thus, although the ordering of interlayer cations is confirmed, the tetrahedrally co-ordinated cations are disordered, and local charge-balance does not exist. The analyzed tetrahedral composition, $Si_{3.0}Al_{1.0}$, is consistent with a mean *T*–0 length of 1.651 Å and the observed angle of rotation of tetrahedra of 5.5°. The basal oxygen atoms have rotated in directions that tend to shorten both the O_b–OH hydrogen-bond contacts and the O_b–M_t distances (M_t: octahedral cation in the 2:1 "talc" sheet). These OH and M_t atoms coincide in a [001]* projection, and the O_b atoms have moved in between at an intermediate *z* level. This is a very favorable stability-factor, created by the stacking sequences of sheets and realized also only in II*b* chlorite.

The H^+ protons are located at 0.81 to 0.96 Å from the centres of their oxygen hosts, and the three surface OH groups form slightly bent (153° to 177°) hydrogen bonds of length 2.91–2.92 Å to the adjacent oxygen surface.

The interlayer octahedral sites are more distorted than the octahedral sites within the 2:1 layer, as judged by the RMS deviation of both the 15 anion–cation–anion angles and the 36 anion–anion–anion angles from the ideal values (Table 5), with site *M*(3) more distorted than *M*(4). The interlayer sheet is considerably thinner than the 2:1 octahedral sheet because of the smaller and higher-charge cations present.

The anisotropic thermal ellipsoids (Table 3) of all cations and of the anions of octahedra of the 2:1 layer are oriented with their major axes quasinormal to the layers. The major axes for the basal oxygen atoms and the interlayer anions, on the other hand, are all in the plane of the layer. Those of the basal oxygen atoms are normal to the *T*–O bonds, and this anisotropy is believed to represent true thermal vibration. The major axes for the ellipsoids of the interlayer hydroxyl groups are quasiparallel to the adjacent H^+ vectors in projection. The large values of B_{equiv} (Table 1) and the anisotropic ellipsoid displacements (Table 3) for the basal oxygen atoms are considered to be due to positional disorder of the tetrahedrally co-ordinated cations.

Ordering of interlayer cations that places a trivalent element in one specific site has been shown by calculations of electrostatic energy (Bish & Giese 1981) to enhance the stability of II*b* chlorite greatly, and the same may be true of I*a* chlorite independent

TABLE 4. BOND LENGTHS (Å) AND ANGLES (°)

Tetrahedron T(1)

T(1)—0(1)	1.634(3)	0(1)—0(3)	2.709(4)	0(1)—T(1)—0(3)	111.0(1)
0(3)	1.654(3)	0(4)	2.706(4)	0(4)	110.9(1)
0(4)	1.653(3)	0(5)	2.713(4)	0(5)	111.0(1)
0(5)	1.658(3)	0(3)—0(4)	2.675(4)	0(3)—T(1)—0(4)	108.0(2)
Mean	1.650	0(5)	2.677(4)	0(5)	107.8(2)
		0(4)—0(5)	2.676(4)	0(4)—T(1)—0(5)	107.9(2)
		Mean	2.693	Mean	109.4

Tetrahedron T(2)

T(2)—0(2)	1.635(3)	0(2)—0(3)	2.710(4)	0(2)—T(2)—0(3)	110.8(1)
0(3)	1.656(3)	0(4)	2.710(4)	0(4)	110.8(1)
0(4)	1.658(3)	0(5)	2.711(4)	0(5)	110.9(1)
0(5)	1.657(3)	0(3)—0(4)	2.678(4)	0(3)—T(2)—0(4)	107.9(2)
Mean	1.652	0(5)	2.684(4)	0(5)	108.2(2)
		0(4)—0(5)	2.684(4)	0(4)—T(2)—0(5)	108.2(2)
		Mean	2.706	Mean	109.5

a b c	a—b	b—c	∠ a-b-c
OH(1)—H(1)	0.963	—	—
OH(2)—H(2)—0(3)	0.863	2.912(4)	153.1(2)
OH(3)—H(3)—0(5)	0.895	2.912(4)	176.7(2)
OH(4)—H(4)—0(4)	0.809	2.916(4)	164.8(2)

Octahedra in 2:1 Layer

	M(1)	M(2)		M(1) lateral	M(2) lateral	M(1)—M(2) sh. diag.		M(2)—M(2) sh. diag.
M—0(1)	2.089(3)x2	2.087(3) 2.091(3)	0(1)—0(2)	3.079(4)x2	3.082(4) 3.077(4)	2.827(4)x2	0(1)—0(1)	2.824(5)
0(2)	2.092(3)x2	2.089(3) 2.084(3)	OH(1)	3.080(4)x2	3.080(4) 3.079(4)	2.792(4)x2	0(2)—0(2)	2.826(6)
OH(1)	2.068(3)x2	2.068(3) 2.069(3)	0(2)—OH(1)	3.085(4)x2	3.077(4) 3.077(4)	2.791(4)x2	OH(1)—OH(1)	2.753(6)
Mean	2.083	2.081	Mean	3.081	3.079	2.803		2.801

Octahedra in Interlayer Sheet

	M(3)	M(4)		M(3) lateral	M(4) lateral	M(3)—M(4) sh. diag.		M(3)—M(3) sh. diag.
M—OH(2)	2.078(3) 2.060(3)	2.006(3)x2	OH(2)—OH(3)	3.098(4) 3.144(3)	2.997(4)x2	2.669(4)x2	OH(2)—OH(2)	2.762(6)
OH(3)	2.078(3) 2.057(3)	2.007(3)x2	OH(4)	3.094(3) 3.146(3)	2.999(4)x2	2.671(4)x2	OH(3)—OH(3)	2.761(6)
OH(4)	2.076(3) 2.059(3)	2.009(3)x2	OH(3)—OH(4)	3.092(3) 3.144(3)	3.003(4)x2	2.667(4)x2	OH(4)—OH(4)	2.759(6)
Mean	2.068	2.007	Mean	3.120	3.000	2.669	Mean	2.761

TABLE 5. OTHER STRUCTURAL PARAMETERS

Sheet thicknesses:

tetrahedral	2.240 Å	τ_{tet}:	T(1)	111.0°
octahedral	2.167		T(2)	110.8°
interlayer	2.031			
0—OH separation	2.827			

Rotation $\alpha_{tet} = 5.5°$

Octahedral distortions:	M(1)	M(2)	M(3)	M(4)
RMS deviation 15 cation angles from ideal	4.85	4.85	7.42	5.98
RMS deviation 36 anion angles from ideal	3.36	3.36	5.28	4.20
rotation σ_{oct}	0.00°	0.06°	2.54°	0.00°
flattening ψ_{oct}	58.7°	58.7°	60.6°	59.6°

Intralayer shift $= -0.334a_3$ $\quad\beta_{obs} = 97.08°$

Layer offset $= +0.333b_2$ $\quad\beta_{ideal} = 97.07°$

Resultant $= -0.334a_1$

of any tetrahedral ordering. Diffuse non-Bragg X-ray scattering by I*a* vermiculite from Kenya has been interpreted by Alcover *et al.* (1973) to indicate the presence of a superlattice (3*a* × *b*) due to ordered interlayer-cations in three different sets of local domains. It is possible that these may interact with the local domains of short-range ordering of tetrahedral cations found by Thompson (1984) in an NMR study of the Llano Co. vermiculite and thereby provide charge balance between layer and interlayer either within domains or between domains in vermiculite. Whether short-range ordering of tetrahedrally co-ordinated cations accompanies the long-range ordering of interlayer cations found here in I*a* chlorite remains to be tested. Charge balance between layer and interlayer is geometrically impossible in the more abundant I*b* and II*b* chlorites, however, so that at best, it can be only a minor factor in chlorite stability.

ACKNOWLEDGEMENTS

This research has been supported in part by grant EAR-106124 from the National Science Foundation and in part by grant 15932-AC2-C from the Petroleum Research Fund, administered by the American Chemical Society.

REFERENCES

ALCOVER, J.F., GATINEAU, L. & MÉRING, J. (1973): Exchangeable cation distribution in nickel- and magnesium-vermiculite. *Clays Clay Minerals* **21**, 131-136.

BAILEY, S.W. & BROWN, B.E. (1962): Chlorite polytypsium. I. Regular and semi-random one-layer structures. *Amer. Mineral.* **47,** 819-850.

BISH, D.L. & GIESE, R.F., JR. (1981): Interlayer bonding in IIb chlorite. *Amer. Mineral.* **66,** 1216-1220.

BROWN, B.E. & BAILEY, S.W. (1963): Chlorite polytypism. II. Crystal structure of a one-layer Cr-chlorite. *Amer. Mineral.* **48,** 42-61.

CROMER, D.T. & MANN, J.B. (1968): X-ray scattering factors computed from numerical Hartree–Fock wave functions. *Acta Cryst.* **A24,** 321-324.

DE LA CALLE, C., DUBERNAT, J., SUQUET, H., PEZERAT, H., GAULTIER, J. & MAMY, J. (1976): Crystal structure of two-layer Mg-vermiculite and Na, Ca-vermiculites. *In* Proc. Int. Clay Conf. (Mexico City), 201-209.

NORTH, A.C.T., PHILLIPS, D.C. & MATHEWS, F.S. (1968): A semi-empirical method of absorption correction. *Acta Cryst.* **A24,** 351-359.

SHIROZU, H. & BAILEY, S.W. (1965): Chlorite polytypism. III. Crystal structure of an orthohexagonal iron chlorite. *Amer. Mineral.* **50,** 868-885.

______ & ______ (1966): Crystal structure of a two-layer Mg-vermiculite. *Amer. Mineral.* **51,** 1124-1143.

THOMPSON, J.G. (1984): ^{29}Si and ^{27}Al nuclear magnetic resonance spectroscopy of 2:1 clay minerals. *Clay Minerals* **19,** 229-236.

Received June 27, 1985, revised manuscript accepted November 28, 1985.